Roughness effects on the electrical conductivity of thin films grown in a quasi-layer-by-layer mode

G. Palasantzas* and J. Th. M. De Hosson
Department of Applied Physics, Materials Science Center, University of Groningen, Nijenborgh 4, 9747 AG Groningen, The Netherlands
(Received 12 July 2000; revised manuscript received 18 October 2000; published 12 March 2001)

We investigate morphology effects on the electrical conductivity on thin semiconducting and metallic films grown in a quasi-layer-by-layer growth mode within the framework of quantum-mechanical electron transport theory. The film growth mode is described by a nonequilibrium Sine–Gordon model that incorporates evaporation/recondensation, surface diffusion, and lattice pinning effects. For semiconducting films, pinning effects manifest themselves as oscillations superimposed on a smoothly increasing conductivity with growth time. For metallic films, quantum size effect oscillations are strongly convoluted with pinning induced oscillations, which dominate the conductivity variations at later stages of growth.

DOI: 10.1103/PhysRevB.63.125404 PACS number(s): 73.50.−h, 72.10.Fk, 73.50.Dn

I. INTRODUCTION

Deviations of thin film surfaces/interfaces from flatness have strong influence on their electrical transport properties, since they induce additional electron scattering.[1–7] Electron scattering by random roughness alters the size and shape of quantum size effects (QSE) in a manner that depends strongly on the form of the corresponding roughness correlation function associated with the nature of roughness at short and long roughness wavelengths.[3,5] In addition, the film growth mode as well as cross-correlation roughness effects can also strongly influence the conductivity of thin films.[7]

At any rate, a layer-by-layer growth mode would eliminate additional electron scattering due to surface roughness. Indeed, at high temperature molecular beam epitaxy or atomic layer epitaxy, the growth in a layer-by-layer mode is anticipated where each depositing layer is completed before the growth of the next layer starts.[6,8] Nevertheless, such a growth mode does not always takes place. Instead, a quasi-layer-by-layer is expected where some nucleation on top of already existing islands can commence, which is, however, only a small portion compared to the bottom grown layer. In systems where layer-by-layer growth or quasi-layer-by-layer growth[6,8] commences, QSE oscillations have been shown to be altered by surface/interface roughness convoluted by oscillations imposed by morphology characteristics.[7]

For example, conductivity measurements in Pb and Pb–In alloyed films grown on Si(111)6×6-Au and Au films on Si(111)7×7,[6] where quasi-layer-by-layer growth occurs showed oscillations with 1 ML (monolayer) period associated with periodic changes in roughness, and were consistent with reflection high energy electron diffraction (RHEED) measurement. Moreover, an additional oscillation of 2 ML-period was observed which was associated with QSE oscillations. In addition, oscillations in resistivity versus film thickness have been observed in Pt films,[9] and Ag, In, Ga films grown on thick Ag and Au basis layers.[10]

In this paper, we perform a theoretical investigation of the quasi-layer-by-layer grown morphological effects on the thin film conductivity convoluted with QSE. The quasi-layer-by-layer mode will be described in terms of a Sine–Gordon (SG) model that incorporates both surface relaxation by surface diffusion and/or evaporation/recondensation. Complications of convolution of QSE and morphology oscillations will be investigated thoroughly for semiconducting and metallic films through a quantum-mechanical Boltzmann approach[3–5] that allows calculation of thin film conductivity influenced solely by electron boundary roughness scattering.

II. CONDUCTIVITY THEORY AND QUASI-LAYER-BY-LAYER GROWTH MODEL

Conductivity formalism

In the Born approximation, the in-plane electrical conductivity of thin films bounded solely by roughness electron scattering is given by[3,5]

$$\sigma=\frac{e^2\hbar^3}{m^2\langle h\rangle}\sum_{n=1}^{N}\sum_{n'=1}^{N}q_n^2q_{n'}^2[C^{-1}]_{nn'}, \tag{1}$$

$$C_{nn'}(E_F)=\int_0^{2\pi}\left\{\delta_{nn}A_nk_n^2\sum_{m=1}^{N}A_m\langle|h(q_{nm},t)|^2\rangle - A_nA_{n'}\langle|h(q_{nn'},t)|^2\rangle\cos\theta\right\}d\theta, \tag{2}$$

where $q_{nn'}=(q_n^2+q_{n'}^2-2q_nq_{n'}\cos\theta)^{1/2}$, $q_n=[(2m/\hbar^2)(E_F-E_n)]^{1/2}$ with E_F and E_n being, respectively, the Fermi energy and the energy minimum of the n miniband edge, and $A_n=|\Phi_n(\langle h\rangle/2)|^2$ with $\Phi_n(z)$ the quantized electron wave function along the z axis for a flat film. N is the number of electron populated lateral subbands and $h(q,t)$ the surface roughness fluctuation from flatness. For a flat film of thickness $\langle h\rangle$ and carrier density n, E_F, and N are determined by the condition[5] $n\langle h\rangle=(m/\pi\hbar^2)(NE_F\rightarrow\Sigma_{n=1,N}E_n)$ with $n_s=n\langle h\rangle$ the areal electron density. If, for simplicity, the electrons are localized in the film by an infinite confining potential well, then $A_n=\hbar^2\pi^2n^2/m\langle h\rangle^3$ and $E_n=(\hbar^2/2m)(n\pi/\langle h\rangle)^2$.[3,5] Clearly the knowledge of the roughness spectrum $\langle|h(q,t)|^2\rangle$ is required to further calculate the electron conductivity from Eqs. (1) and (2).

Growth model

A quasi-layer-by-layer growth can be described by a phenomenological Langevin equation representing the nonequilibrium analogue of the SG model[11–13]

$$\frac{\partial h(\mathbf{r},t)}{\partial t} = R + \nu\nabla^2 h - \kappa\nabla^4 h + \eta(\mathbf{r},t) - A\sin\left[\frac{2\pi h(\mathbf{r},t)}{c}\right], \tag{3}$$

with $h(\mathbf{r},t)$ the surface height, R the rate of impinging adatoms, ν the evaporation/recondensation coefficient, and κ the diffusion coefficient. $\eta(\mathbf{r},t)$ represents intrinsic random noise fluctuations of amplitude D such that $\langle \eta(\mathbf{r},t)\,\eta(\mathbf{r}',t')\rangle = 2D\,\delta(\mathbf{r}-\mathbf{r}')\,\delta(t-t')$ and $\langle \eta(\mathbf{r},t)\rangle = 0$ which are responsible for roughening during growth. A is the strength of the pinning term that favors energetically integer values of surface heights in units of the atomic spacing c.[11,13]

Indeed, the pinning force $V_{\rm pin} = -A\sin[2\pi h(\mathbf{r},t)/c]$ mimics qualitatively two-dimensional (2D) nucleation-dominated growth process. For low surface coverage, such that $V_{\rm pin} < 0$, there are a few atoms on the top layer and thus the possibility of 2D islands to overcome the potential barrier to reach the critical island size is small. As a result a number of deposited atoms that are not stable on the crystal surface will evaporate back into the vapor phase. With increasing surface coverage such that $V_{\rm pin} > 0$, on the surface there are many 2D islands leading to an enhanced probability that monomers to be attached to islands resulting in an easier growth process.[12,13] For a small pinning force $V_{\rm pin} = -\varepsilon A\sin[2\pi h(\mathbf{r},t)/c]$, Eq. (3) can be solved perturbatively and the roughness spectrum $\langle|h(\mathbf{q},t)|^2\rangle$ is given by (see Appendix)

$$\begin{aligned}\langle|h(\mathbf{q},t)|^2\rangle = {} & D\frac{1-e^{-2(\kappa q^4+\nu q^2)t}}{\kappa q^4+\nu q^2} \\ & + \frac{ADc}{\pi R}\frac{e^{-2(\kappa q^4+\nu q^2)t}}{\kappa q^4+\nu q^2}\sin(2\pi Rt/c) \\ & - 4AD\frac{\cos(2\pi Rt/c) - e^{-2(\kappa q^4+\nu q^2)t}}{(2\pi R/c)^2 + 4(\kappa q^4+\nu q^2)^2} \\ & - \frac{4AD}{c(\kappa q^4+\nu q^2)}\frac{\sin(2\pi Rt/c)}{(2\pi R/c)^2+4(\kappa q^4+\nu q^2)^2},\end{aligned} \tag{4}$$

which is what is required in the calculation of the film electrical conductivity.[3]

III. RESULTS AND DISCUSSION

Our conductivity calculations (unless stated) were performed for growth rate $R = 3$ Å/s, $D = 0.2$ Å/s, and $c = 3$ Å, as well as the units of the coefficients ν and κ are assumed such that $[\nu] = $ Å^2/s and $[\kappa] = $ Å^4/s. In addition, we note that the contribution of evaporation/recondensation in surface relaxation is significant at larger length scales ($r > 2\pi\sqrt{\kappa/\nu}$), while the shorter length scales ($r < 2\pi\sqrt{\kappa/\nu}$) surface diffusion is the dominant one.

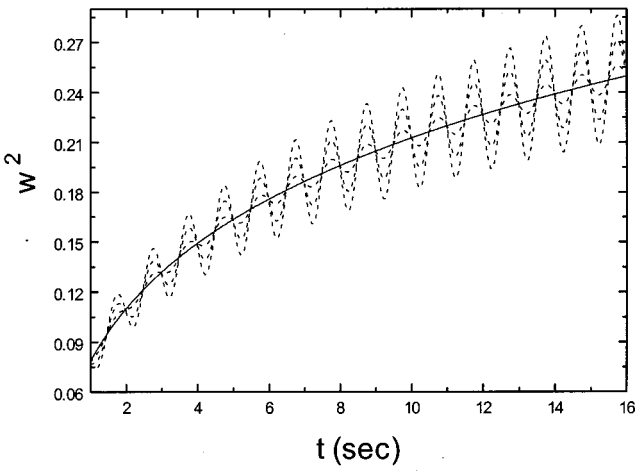

FIG. 1. (a) Roughness amplitude $w(t)$ vs evolution time t for pinning amplitude $A = 0$, 0.1, 0.3, and 0.5, $D = 0.2$, $\nu = 1$, and $\kappa = 5$. With increasing A the oscillation amplitude increases.

Figure 1 shows calculations of the time evolving rms roughness amplitude

$$w(t) = \langle h^2\rangle^{1/2} = \int_{0<q<\pi/c}\langle|h(q,t)|^2\rangle q\,dq$$

for various values of the pinning strength coefficient A. In both cases, as the pinning strength A increases, the oscillation amplitude of $w(t)$ increases superimposed on a growing roughness amplitude due to kinetic roughening. The position of these oscillations is the same since only A changes. The oscillatory behavior for $A > 0$ is also characteristic for the roughness spectrum $\langle|h(\mathbf{q},t)|^2\rangle$, as can be seen in Fig. 2 for $q = q_c = (8\pi n_s)^{1/2}$ with $n_s = 4.8\times10^{-4}$ Å^{-2} reflected in the corresponding statistical properties, such as $w(t)$. For the parameters used in the calculations $w(t)/Rt \ll 1$, which is an important constraint not only for the justification of the perturbative solution of the SG model given by Eq. (3) but also the necessary condition for the validity of the conductivity formalism, which, in general, requires $w \ll \langle h\rangle$[3,4] in order for electron localization effects in the x-y plane to be ignored.

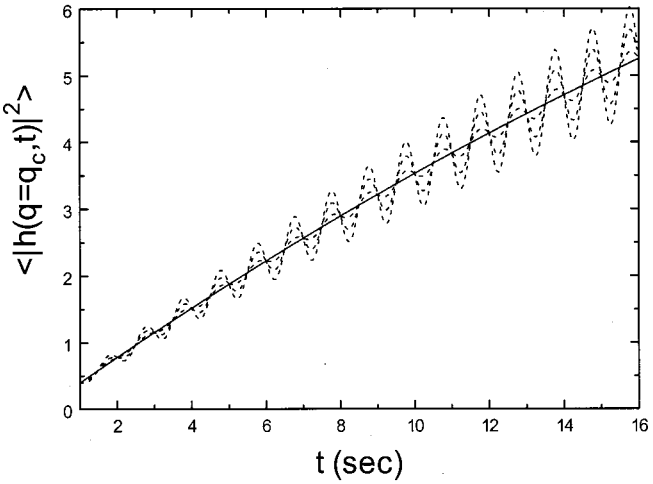

FIG. 2. Power spectrum vs evolution time t for $\nu = 1$, $\kappa = 5$, $A = 0$, 0.1, 0.3, 0.5 for $q = q_c = (8\pi n_s)^{1/2}$ with $n_s = 4.8\times10^{-4}$ Å^{-2}.

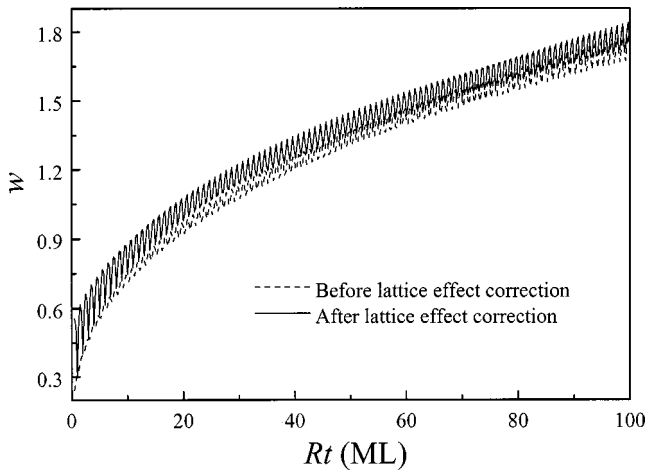

FIG. 3. Roughness amplitude w vs evolution time t with and without discrete lattice effect correction for $A=0.2$, $D=0.5$, $R=3$, $c=3$, $\kappa=2$, $\nu=0$ (diffusion dominated surface relaxation). The roughness amplitude increases almost linearly with time with an oscillating growth rate of small amplitude since $R \gg A$.

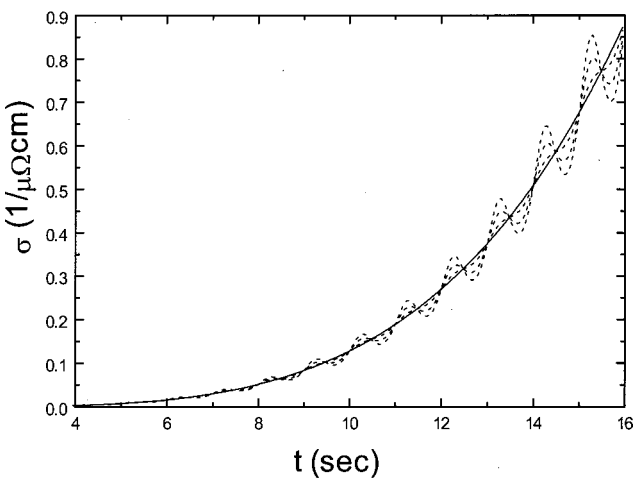

FIG. 4. Conductivity σ vs evolution time t for semiconducting films with areal electron $n_s=4.8\times10^{-4}$ Å^{-2}, $D=0.2$, $\nu=1$, $\kappa=5$, and $A=0$ (solid line), 0.1, 0.3, 0.5.

Nevertheless, we should point out that the oscillatory behavior is smaller at the early stages of growth. This is due to the fact that Eq. (1) is a continuous model. As a result, discrete lattice effects are ignored. Indeed, as long as the surface coverage $\theta\{=\langle h\rangle - \mathrm{in}[\langle h\rangle/c]c\}$ is not an integer, the surface will be rough independent of the smoothing mechanism. Such a process is highly washed out at very early stages of growth. Such an effect can be corrected by considering the fact that the 2D-nucleation growth mode and dynamic roughening are independent, which allows to consider as an effective interface width $w \equiv \sqrt{w^2+w_{\mathrm{dis}}^2}$ with $w_{\mathrm{dis}}^2 = c\,\theta(1-\theta)$. Figure 3 shows the influence of the discrete lattice effect correction, which leads to recovery of the oscillatory behavior at early growth stages. At later growth stages, the Langevin equation dominates the description of roughening[13] allowing its use for electron transport calculations.

Semiconducting film conductivity

When the number of occupied lateral minibands is small (e.g., $N=1,2$), the film is termed as semiconducting. For only one lateral miniband populated ($N=1$) there are no quantum size effects present. In this case, only intraminiband scattering contributes to the conductivity simplifying the understanding of pinning effects on the conductivity dependence with increasing growth time. As a result, an oscillatory behavior present will arise solely from morphology effects associated in the present case to pinning effects favoring a layer-by-layer growth.

Figure 4 shows the temporal dependence of the conductivity for sufficiently low areal electron density $n_s=4.8\times10^{-4}$ Å^{-2} in such a way that only one miniband is populated for the thicknesses or growth times considered. In the absence of a pinning force, $A=0$, as shown by the solid line, the conductivity increases with growth time following a simple power law behavior $\sigma \propto t^X$ with $X=X(\nu,\kappa)$ and depending on the strength of the relaxation mechanisms, namely evaporation/recondensation and surface diffusion in the present case. However, as pinning starts to contribute for $A>0$, additional oscillations occur and are superimposed on the conductivity increment that occurs in an oscillatory manner. With increasing pinning strength A, the conductivity oscillation amplitude increases especially at latter stages of growth. Nevertheless, the existence of the initial transient regime, where the continuum equation washes out discrete lattice effects (see Fig. 3), is also pronounced for the conductivity besides that of morphological roughness parameters such as the rms roughness amplitude w (Fig. 1).

In order to gain further understanding on the effect of pinning on the conductivity, we consider the following. For one miniband occupied ($N=1$), the conductivity is given by[5]

$$\sigma = \frac{2n_s e^2}{\hbar \pi^3}\langle h\rangle^5 \left[\int_0^{2\pi} \langle |h(q_{11},t)|^2\rangle (1-\cos\theta)\,d\theta\right]^{-1} \quad (5)$$

with $q_{11}=[4\pi n_s(1-\cos\theta)]^{1/2}$ for an infinite potential well.[5] Equation (5) shows that the spatial frequency regime of the morphology with wave vectors $0<q<q_c=(8\pi n_s)^{1/2}$ will contribute to the film conductivity. This is due to the fact that forward scattering, which contributes less to the conductivity, occurs for $\theta=0$ or 2π yielding $q_{11}=0$, while backward scattering has the largest contribution to the conductivity for $\theta=\pi$ yielding $q_{11}=q_c=(8\pi n_s)^{1/2}$. For forward scattering the integrand in the integral part of Eq. (5) becomes

$$\lim_{\theta\to 0,2\pi}\langle |h(q_{11},t)|^2\rangle (1-\cos\theta) = [(ADc/\pi R)-(ADc/\pi^2 R^2)]\sin(2\pi Rt/c)$$

which has a positive amplitude $[(ADc/\pi R)-(ADc/\pi^2R^2)]\rangle>0$ for $R>1/\pi$. For backward scattering we obtain $\langle |h(q_{11}=q_c,t)|^2\rangle(1-\cos\pi)=2\langle |h(q_{11}=q_c,t)|^2\rangle$ which is always positive independently of the deposition rate R. Therefore, depending on the deposition rate, the contribution of backward and forward scattering on the pinning induced morphological oscillations could be in-phase for sig-

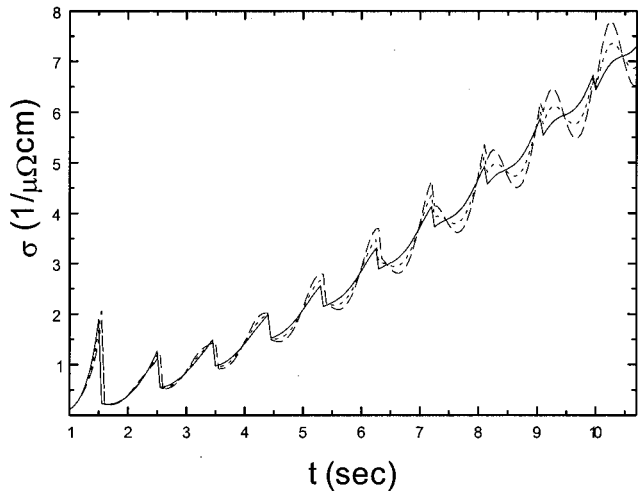

FIG. 5. Conductivity σ vs evolution time t for metallic films with bulk electron density $n=13.2\times10^{-2}$ Å^{-3}, $D=0.2$, $\nu=1$, $\kappa=5$, and $A=0$ (solid line), 0.1, 0.3, 0.5.

nificant deposition rates $R>1/\pi$ or out-of-phase for very low deposition rates, such that $R<1/\pi$. Figure 2 shows the behavior of the roughness spectrum for backward scattering, which has the strongest contribution to the conductivity. Clearly it can be seen that at the early stages of growth, the morphological oscillations arising from pinning are rather weak, thus implying a weak contribution to the conductivity, and vice versa upon inclusion of the discrete lattice effect correction, which is depicted in Fig. 3.

Metallic film conductivity

For metallic films the number of occupied minibands increases rapidly with increasing thickness or growth time ($N\gg1$), leading alternatively to the presence of QSE oscillations. These oscillations arise from the fact that each time the Fermi level crosses the bottom of a lateral miniband another channel for scattering opens, which reduces the conductivity and further leads to an oscillatory increment. In general, their shape and size depends on the particular rough morphology under consideration as previous studies have shown.[3,5,7] The situation for metallic films is more complex than that of semiconducting films; since besides intraminiband scattering, transitions between lateral minibands leading to interminiband scattering yield significant contributions the conductivity behavior [cross-terms in Eq. (2)].

As can be seen in Fig. 4 by the solid line, in the absence of pinning or $A=0$, the QSE oscillations have a saw-tooth structure with increasing growth time and a period $\sim\lambda_F/2$ with λ_F the Fermi wavelength. As long as pinning starts contributing to conductivity, the shape and magnitude of the oscillations start to deviate from the pure QSE oscillatory behavior (absence of pinning; $A=0$), and rather interpenetrate through these pure QSE oscillations. The effect of pinning, in comparison to the case of semiconducting films shown in Fig. 5, starts to appear even at very early stages of growth and progressively prevails over the pure QSE mode with increasing growth time. In addition, with increasing surface relaxation (increasing coefficient v and/or k) the amplitude of pinning induced oscillations increases, as is depicted in Fig. 6.

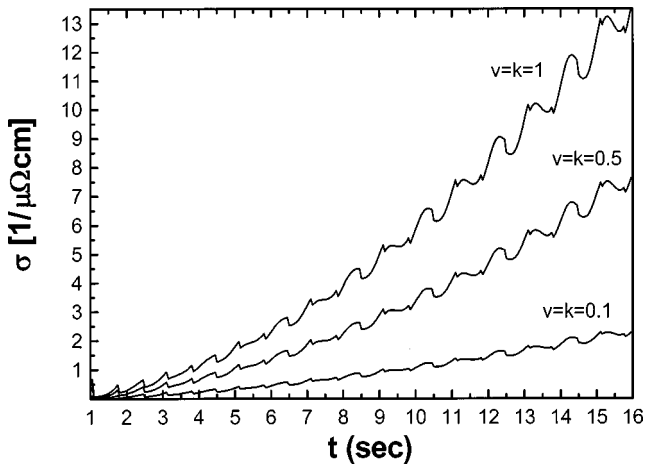

FIG. 6. Conductivity σ vs evolution time t for metallic films with bulk electron density $n=13.2\times10^{-2}$ Å^{-3}, $D=0.2$, $\nu=\kappa=0.1$, 0.5, 1, and $A=0.2$.

At later growth stages where the effect of pinning appears to be more pronounced within the continuum model description, the conductivity oscillations bear similarities with those of the semiconducting case indicating a strong dominance of morphological effects over quantum effects arising from the electron confinement in the direction perpendicular to the film surface. In Fig. 7 we present conductivity calculations for various bulk electron densities in the range $n=13.2\times10^{-4}$–13.2×10^{-2} Å^{-3}. With lower electron density the number of populated lateral minibands decreases leading to less QSE oscillations, and as a result, to reduced contribution of inter-miniband scattering. Comparing Figs. 5 and 7, we can infer that in the latter case, pinning induced oscillations are more affected by QSE oscillations complicating the interpretation of the conductivity behavior altered by morphology effects.

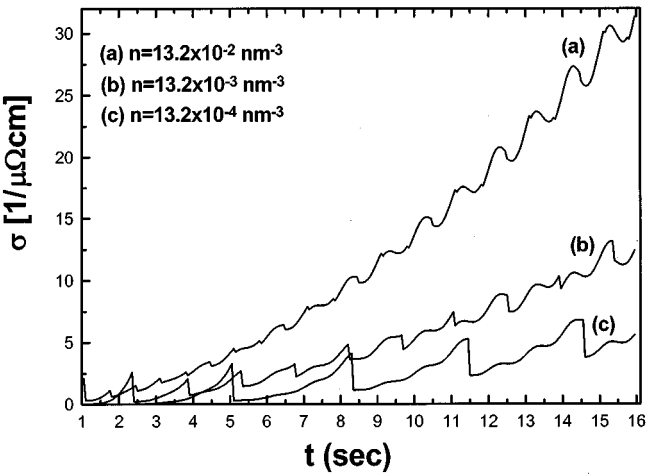

FIG. 7. Conductivity σ vs evolution time t for metallic films with various bulk electron densities, as indicated for $R=3$, $c=3$, $A=0.2$, $k=5$, and $v=2$.

IV. CONCLUSIONS

In conclusion, we investigated roughness effects on the electrical conductivity on thin semiconducting and metallic films grown in a quasi-layer-by-layer growth mode within the framework of Boltzmann quantum-mechanical electron transport theory. The film growth mode was described in terms of a nonequilibrium Sine-Gordon model that incorporates roughening and surface relaxation in terms of evaporation/recondensation and surface diffusion, combined with lattice pinning effects that favor layer-by-layer growth. The latter type of growth effect manifests itself on the temporal evolution of roughness parameters, such as the rms roughness amplitude. For semiconducting films, pinning effects manifest themselves as oscillations on an otherwise smoothly increasing conductivity with growth time in the absence of pinning. However, for metallic films, quantum size effect oscillations are convoluted with morphological oscillations leading to complex oscillatory patterns of the conductivity versus thickness or growth evolution time. Clearly for metallic films, pinning induced oscillations at later stages of growth dominate the conductivity behavior over quantum mechanical induced oscillations (QSE). At any rate, we should point out that our results are limited to late stages of growth thus minimizing the effect of neglecting discrete lattice effects (Fig. 3). Further studies are in progress to properly incorporate discrete lattice effects in quantum mechanical thin film conductivity calculations.

ACKNOWLEDGMENTS

We would like to acknowledge support from the Netherlands Institute for Metals Research, and important correspondence with Dr. Y.-P. Zhao from Renselaer Polytechnic Institute for communicating his calculations on pinning effects on rough growth fronts prior to publication,[13] as well as providing Fig. 3 to illustrate discrete lattice effects. Moreover, we would like to acknowledge useful discussions with J. Barnas.

APPENDIX

If we assume the perturbative expansion $h=h_1+\varepsilon h_2+\varepsilon^2 h_3+\ldots$, Eq. (3) yields

$$\frac{\partial h_1}{\partial t}=R+\nu\nabla^2 h_1-k\nabla^4 h_1+n;$$

$$\frac{\partial h_2}{\partial t}=\nu\nabla^2 h_2-k\nabla^4 h_2-A\sin\left(\frac{2\pi h_1}{c}\right)+n. \tag{A1}$$

By setting $h_1=h_{1,0}+h_{1,1}$ with $h_{1,0}=Rt$, we obtain from Eq. (A1)

$$h_{1,1}(\mathbf{q},t)=\int_0^t n(\mathbf{q},\tau)e^{-(kq^4+\nu q^2)(t-\tau)}d\tau \tag{A2}$$

with $h_{1,0}$ and $h_{1,1}$ representing, respectively, the average surface height and the height fluctuation at zero-order perturbation. Since usually $\langle h_{1,1}^2\rangle \ll h_{1,0}$, the pinning-sine term in Eq. (A1) can be further approximated by

$$\frac{\partial h_2}{\partial t}=\nu\nabla^2 h_2-k\nabla^4 h_2-A\sin\left(\frac{2\pi R}{c}t\right)-\frac{2\pi A}{c}h_{1,1}\cos\left(\frac{2\pi R}{c}t\right). \tag{A3}$$

Therefore, if we set $h_2=h_{2,0}+h_{2,1}$ such that

$$\frac{\partial h_{2,0}}{\partial t}=-A\sin\left(\frac{2\pi R}{c}t\right),$$

$$\frac{\partial h_{2,1}}{\partial t}=\nu\nabla^2 h_{2,1}-k\nabla^4 h_{2,1}-\frac{2\pi A}{c}h_{1,1}\cos\left(\frac{2\pi R}{c}t\right) \tag{A4}$$

and integrate, we obtain the average film thickness $\langle h\rangle = h_{1,0}+h_{2,0}$

$$\langle h\rangle = Rt+\frac{Ac}{2\pi R}\left[\cos\left(\frac{2\pi R}{c}t\right)-1\right] \tag{A5}$$

and

$$h_{2,1}(\mathbf{q},t)=-A\int_0^t h_{1,1}(\mathbf{q},\tau)\cos(2\pi R\tau/c)e^{-(kq^4+\nu q^2)(t-\tau)}d\tau, \tag{A6}$$

which finally yields the roughness spectrum of Eq. (4).

*Corresponding author. Electronic mail: G.Palasantzas@phys.rug.nl

[1] T. Ando, A. B. Fowler, and F. Stern, Rev. Mod. Phys. **54**, 437 (1982); A. Hartstein, T. H. Ning, and A. B. Fowler, Surf. Sci. **58**, 178 (1976); T. Ando, Jpn. J. Phys. **51**, 3900 (1982).

[2] J. C. Hensel, R. T. Tung, J. M. Poate, and F. C. Unterwald, Phys. Rev. Lett. **54**, 1840 (1985); P. A. Badoz, A. Briggs, E. Rosencher, A. A. d' Avitaya, and C. d'Anterroches, Appl. Phys. Lett. **51**, 169 (1985); J. Y. Duboz, P. A. Badoz, E. Rochencher, J. Henz, M. Ospelt, H. von Kanel, and A. A. Briggs, *ibid.* **53**, 788 (1988); R. G. P. van der Kraan, J. F. Jongste, H. M. Laeger, G. c. A. M. Janssen, and S. Radelaar, Phys. Rev. B **44**, 13 140

(1991).
[3] G. Fishman and D. Calecki, Phys. Rev. Lett. **62**, 1302 (1989); G. Fishman and D. Calecki, Phys. Rev. B **43**, 11 581 (1991); J. Barnas and Y. Bruynseraede, Europhys. Lett. **32**, 167 (1995); J. Barnas and Y. Bruynseraede, Phys. Rev. B **53**, 5449 (1996).
[4] H. Sakaki, T. Noda, K. Hirakawa, M. Tanaka, and T. Matsusue, Appl. Phys. Lett. **51**, 1934 (1987); A. Gold, Z. Phys. B: Condens. Matter **74**, 2100 (1989).
[5] G. Palasantzas and J. Barnas, Phys. Rev. B **56**, 7726 (1997); G. Palasantzas and J. Barnas, Phys. Status Solidi B **209** , 319 (1998); J. Barnas and G. Palasntzas, J. Appl. Phys. **82**, 3950 (1997).
[6] M. Jolocowvski and E. Bauer, Phys. Rev. B **38**, 5272 (1988); M. Jolocowvski, E. Bauer, H. Knoppe, and G. Lilienkamp, *ibid.* **45**, 13 607 (1992); M. Jolocowvski, M. Hoffmann, and E. Bauer, Phys. Rev. Lett. **76**, 4227 (1996); M. Jolocowvski and E. Bauer, Phys. Rev. B **37**, 8622 (1988).
[7] G. Palasantzas, Y.-P. Zhao, G.-C. Wang, T.-M. Lu, and J. Th. M. De Hosson, Phys. Rev. B **61**, 11 109 (2000).
[8] F. Rosenberger, in *Interfacial Aspects of Phase Transformations*, edited by B. Mutaftschiev (Reidel, Dordrecht, 1982).
[9] G. Fischer and H. Hoffmann, Z. Phys. B **39**, 287 (1980); H. Hoffmann and G. Fischer, Thin Solid Films **36**, 25 (1976).
[10] D. Schumacher and D. Stark, Surf. Sci. **123**, 384 (1982).
[11] H.-Y. Yang, G.-C. Wang, and T.-M. Lu, Phys. Rev. B **51**, 17 932 (1995).
[12] P. Nozieres, in *Solid Far From Equilibrium*, edited by C. Godrche (Cambridge University Press, New York, 1991), pp. 135–143.
[13] Y. P. Zhao, G.-C. Wang, and T.-M. Lu, *Characterization of Amorphous and Crystalline Rough Surfaces-Principles and Applications*, Experimental Methods in the Physical Science Vol. 37 (Academic Press, New York, 2000).